10.1109/ULTSYM.2009.0128

Performance of Three-Dimensional Sonoelastography in Prostate Cancer Detection: A Comparison Between *ex vivo* and *in vivo* Experiments

B. Castaneda
Laboratorio de Imágenes Médicas
Pontificia Universidad Católica del Perú
Lima, Perú

K. Hoyt
Department of Radiology
University of Alabama at Birmingham
Birmingham, Alabama, USA

K. Westesson, L. An, J. Yao, L. Baxter, J. Joseph, J. Strang, D. Rubens, K. Parker
Rochester Center for Biomedical Ultrasound
University of Rochester
Rochester, NY, USA

***Abstract*—In this paper, we evaluate and compare the performance of three-dimensional (3D) sonoelastography for prostate cancer detection *ex vivo* and *in vivo*. Ultrasound (US) B-mode and sonoelastographic volumes were acquired from eleven prostate glands before and after radical prostatectomy. Semi-automatic algorithms were used to segment the surface of the gland from the US B-mode volume and the tumors from sonoelastographic data. To assess the detection performance, 3D sonoelastographic findings were compared in size and position to 3D histological data. One gland was discarded due to poor contact. In the remaining ten, both, *in vivo* and *ex vivo* sonoelastography showed similar performance in prostate cancer detection: over 80% accuracy for tumors larger than 4 *mm* in estimated diameter. These results are an improvement over US B-mode but not yet sufficient to replace biopsy. However, 3D sonoelastography has the potential to become an imaging tool to guide biopsies.**

Keywords- Prostate cancer detection; sonoelastography; three-dimensional ultrasound; elasticity imaging.

I. INTRODUCTION

Prostate cancer is an important concern in aging male populations worldwide. In the United States, it is the most prevalent type of cancer in men. It is second in mortality only after lung cancer with 28,660 estimated deaths for 2008 [1]. In Peru, it has the second highest mortality rate after lung cancer [2].

Current prostate cancer diagnosis relies on a combination of digital rectal examination (DRE), blood screening based on prostate specific antigen levels (PSA) and biopsy guided by transrectal ultrasound (TRUS) imaging. However, all of these techniques present disadvantages. DRE may miss tumors in the anterior region of the gland since it is anatomically limited to the posterior part of the prostate [3]. Increased levels of PSA occur due to the presence of cancer and other conditions such as hyperplasia and prostatic inflammation [4]. Finally, tumors may appear as isoechoic in TRUS images. Therefore, random biopsies are required to confirm the presence of cancer [5]. However, a high number of biopsies per patient yields a low number of cancers detected [6]. The shortcomings in sensitivity and specificity of these methods have motivated the research community to look for a novel non-invasive alternative in diagnosis.

DRE is based on the premise that pathological processes produce changes in tissue mechanical properties. Following this idea, imaging the elastic properties of biological tissues has become an area of active research [7,8,9] with some efforts focused on prostate cancer detection [6,10,11,12]. In particular, sonoelastography is a tissue elasticity imaging technique that estimates the amplitude response of tissues under harmonic mechanical excitation using ultrasonic Doppler techniques [13]. This technique qualitatively identifies regions of abnormal stiffness in real time [14] and has been previously applied to prostate cancer detection.

An initial comparison between sonoelastographic images and corresponding histological slides with promising results was reported by Rubens et al. in 1995 [15]. An experimental setup for three dimensional (3D) sonoelastography was built by Taylor and colleagues [16]. Their results using this setup indicated that sonoelastography had the capability to detect lesions over 1cc [6]. More recently, preliminary results with a small number of prostate specimens have been presented including an extension to the *in vivo* imaging of one patient [17]. This previous work, although promising, has mainly focused on *ex vivo* experiments.

This work evaluates the performance of 3D sonoelastography for prostate cancer detection *in vivo* and *ex vivo* and compares their performance. In both cases, semi-automatic algorithms to process US B-mode and sonoelastographic images are used to determine the size and position of tumors in three dimensions. Results are compared to histological volumes to evaluate the overall performance.

This research is sponsored by NIH Grants 5R01 AG016317-6 and 5R01 AG29804-3.

II. METHODS

The *ex vivo* and *in vivo* studies involving human prostate glands presented in this paper were approved by the Institutional Review Board of the University of Rochester Medical Center and compliant with the Health Insurance Portability and Accountability Act. In all cases, it was verified that the patients were not treated with radiation or hormonal therapies which alter the gland stiffness and the amount of residual tumor.

A. In vivo experiments

Eleven patients underwent a TRUS examination the day prior to their scheduled radical prostatectomy. A magnetic tracking device (MiniBird, Ascension Technologies, Burlington, VA, USA) was mounted on the TRUS probe [17] of an specially modified Logiq9 US scanner (General Electric Medical Systems, Milwaukee, WI, USA). This device enabled the reconstruction of 3D US B-mode and sonoelastographic volumes of the prostate gland. The external vibration was induced by a specially designed plate using two mechanical actuators (Buttkicker Concert, The Guitammer Company Inc., Westerville, Ohio, USA) each driven by a low frequency harmonic signal. To select the vibration frequency, a sonoelastographic image of the mid-gland was tested starting at 70Hz and increasing the frequency until attenuation did not permit to obtain a good quality image. The quality was judged in terms of the uniformity of the vibration field filling the prostate. The highest frequency which allowed an image of good quality was selected for further analysis. Deficits in sonoelastographic volumes were identified by achieving a consensus of 3 observers and segmented using the same techniques described in [18] but extended to 3D domain. Discrete dynamic contours were used to outline the boundary of the prostate gland in each of the US B-mode images resulting in a 3D representation of the surface of the gland [19]. The combination of both segmentations formed the *in vivo* volume of the prostate.

B. Ex vivo experiments

Prostate glands from the same eleven patients were received after radical prostatectomy and embedded in a 10.5% gelatin (300 Bloom Pork Gelatin, Gelatin Innovations Inc., Schiller Park, IL, USA) bowl-shaped mold. Vibration was provided by two parallel rigid metal strips positioned underneath the mold. The strips had a rectangular cross section (90 *mm* in length, 6 *mm* in width and 7 *mm* in height) and were connected to an external piston (Vibration Test Systems, Aurora, OH, USA). Input signals to the piston were provided by a harmonic waveform generator (Model 3511A Pragmatic Instruments, San Diego, CA, USA) after amplification (Model 2706, Brüel & Kjaer, Naerum, Denmark). The metals strips were vibrated at a combination of low frequencies (105, 140, 175 and 210 *Hz*) to minimize imaging artifacts resulting from reflections from the boundaries of the mold [16]. Co-registered sonoelastographic and US B-mode volumes were acquired using the modified Logiq 9 US scanner. Images were obtained at 1-*mm* spacing in the longitudinal direction (i.e. prostate apex to base) by mounting a M12L linear array probe on a motorized track (Velmex, Bloomfield, NY, USA). The image plane was normal to the long axis of the metal strips. Segmentations of deficits in the Sonoelastographic data and of the boundary of the gland in US B-mode images were performed similarly to the *in vivo* case to form an *ex vivo* volume.

C. Pathological Processing: Ground Truth

After *ex vivo* imaging, the specimen was weighted and measured to determine the maximum length from apex to base, transversely and anteroposteriorly. A landmark device, which consisted of two sets of four 3-*mm*-diameter mating metal prongs, was inserted longitudinally into the specimen to provide fiducial markers. After fixation, the gland was measured to assess shrinkage, sliced into 4-*mm*-thick sections from the apex to the base, and digitally photographed. Tissues were then transferred to cassettes and embedded in paraffin (Paraplast, Sherwood Medical, St. Louis, MO, USA). The tissue was sliced further into 5-μm-thick sections and placed on glass slides. The microscopic whole-mount sections were examined by a pathologist who was blinded to the results from sonoelastography. Areas of carcinoma and benign prostatic hyperplasia (BPH) were outlined with black and blue marking pens, respectively. Subsequently, a histological volume was created by aligning the digital photographs of each histological slide using the holes from the landmark device as a reference and interpolating the spaces in-between slices. The volume was scaled to compensate for shrinkage.

D. Validation

In order to assess the cancer detection performance, 3D sonoelastographic findings, in both *in vivo* and *ex vivo*, were compared in size and position to the histological volume. First, the *in vivo* and the *ex vivo* volumes were registered independently to the 3D histological data using the surface of the gland as a marker and following a combination of rigid and deformable (b-splines) algorithms [20]. For tumors to match, the ratio of the estimated diameters of the deficit in sonoelastography and the tumor in histology had to be in the range between 50% and 150%. Additionally, their centers of mass had to be less than 15 *mm* apart in the registered space. These criteria were selected to compensate for problems during registration and for the coarse sampling in the histological volume.

III. RESULTS

Out of the 11 scanned prostate glands, 1 case was discarded due to poor contact between the gland and transducer during the *in vivo* experiment. In the remaining cases, *in vivo* sonoelastographic imaging detected 12 tumors. Their average diameter measured 7.4±4 *mm* versus 7.5±3.5 *mm* in the histological volume. The smallest detected tumor had an estimated diameter of 3 *mm*. In addition, 12 other deficits were depicted by sonoelastography. 6 of them corresponded to BPH and the rest remained unexplained. 7 tumors were undetected with an average diameter of 3.8±1.7 *mm*. Fig. 1 illustrates a representative case comparing findings from sagital *in vivo* US B-mode and sonoelastographic images with histology. Sonoelastography shows 3 major deficits, one at the anterior part of the base and two others closer to the apex of the gland.

Axial histological cross-sections confirmed the presence of BPH and cancer.

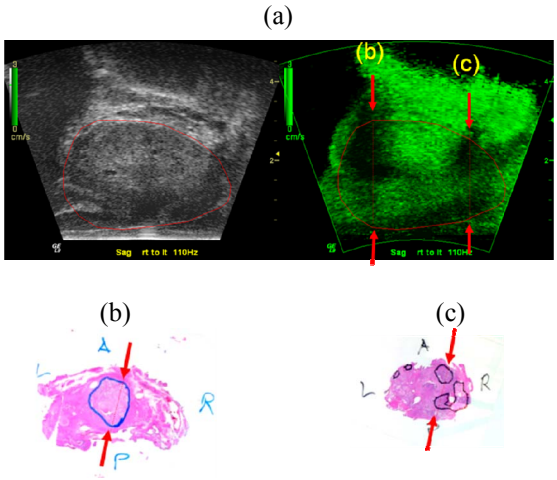

Figure 1. Co-registered US B-mode and sonoelastgraphic images (a) showing a sagital view of an *in vivo* prostate. The gland is outlined in red. The sonoelastographic image presents 3 deficits, one in the base and two in the apex. The red arrows indicate the cross-sections where histological images were taken. The cross-section which is located closer to the base of the galnd (b) presents a BPH nodule in the middle (marked in blue). The cross-section at the apex of the gland shows the presence of cancer marked in black.

Ex vivo sonoelastography found 18 deficits. 9 of these corresponded to cancerous masses, 4 to BPH nodules, and 5 were unexplained false positives. 5 tumors were missed entirely. The average diameter of the detected tumors was 7.2±3.1 *mm* measured in the sonoelastographic images versus 7.5±3.5 *mm* measured on histology. The minimum estimated diameter of a detected tumor was 2.5 *mm*. The undetected tumors measured in average 5.3 ± 3.2 *mm* in diameter. Fig. 2 illustrates a representative case of *ex vivo* sonoelastography. Corresponding US B-mode, sonoelastographic, and histological images are shown. Sonoelastography presents two major deficits to the left and to the right of the gland. Histology shows that one of the deficits corresponds to cancer surrounded by BPH. The other deficit corresponds entirely to BPH.

Fig. 3 presents a comparison of *in vivo* and *ex vivo* sonoelastographic volumes of the same gland against its corresponding histological volume. In both cases, the tumor depicted by sonoelastography coincides with the tumor outlined by the pathologist in the histological volume.

IV. Discussion

The capability of sonoelastography to find cancer depends on the size and elastic contrast of the tumors in comparison with the normal surrounding tissue [14]. In our experiments, the average diameter was less than 8 *mm* and the expected elastic contrast was less than 3 [21]. The small size and low contrast represent adverse conditions for the imaging system. On average, the undetected tumors (false negatives) had 5 *mm* and 3 *mm* in diameter for *ex vivo* and *in vivo* experiments, respectively.

Benign conditions in the prostate, such as BPH and calcifications may manifest as stiffer than normal tissue [22], and therefore, they are a source of false positives in this study. A qualitative imaging tool such as sonoelastography might not be able to distinguish these benign conditions from cancer. A quantitative imaging technique such as crawling wave sonoelastography [23] may provide a better understanding of the visco-elastic properties of these conditions, and therefore, may distinguish them from normal and cancerous tissue.

Artifacts due to how vibration is induced in the tissue are another source of false positives. These artifacts are different in the *in vivo* and in the *ex vivo* cases. In the latter, modal patterns appear due to the destructive interference between the shear wave sources and the reflection from boundaries of the gelatin mold. Although chords (multiple-frequency signals) were used to minimize this effect, they are not sufficient to eradicate them. The experimental setup needs to be adjusted so that either modal patterns are further reduced or that their presence can be determined.

In vivo prostate experiments showed high contrast sonoelastographic images. Furthermore, these images are less affected by modal patterns because of the heterogeneous nature of tissue. However, boundary of internal structures, such as the urethra and calcifications caused artifacts (which were not scored as cancer). Technical pitfalls include the change in the overall attenuation of the ultrasound with the angle of rotation of the probe. This effect manifests as aliasing at lateral margins and incomplete penetration at the mid-gland. Coupling of externally induced mechanical vibrations to the prostate tissue is another major obstacle in obtaining high-quality results *in vivo*.

Higher contrast images, and therefore, a better detection rate of lesions, could be obtained by pushing the sonoelastographic experiments to higher frequencies. However, higher attenuation over long distances will diminish the signal at higher frequencies, so better means of applying local vibration at higher frequencies (approaching 200 *Hz* or higher) need to be developed. In that sense, evaluation of US radiation force as a vibration source is suggested.

Overall, qualitative sonoelastographic imaging presented better results than US B-mode images to detect the presence of tumors, especially when they are larger than 4*mm* in diameter. If only these tumors are considered in the analysis, *in vivo* sonoelastography showed 83% accuracy, 91% sensitivity and 81% specificity, whereas *ex vivo* sonoelastography showed 82% accuracy, 75% sensitivity and 84% specificity. Even though this is an improvement over US B-mode, it is not sufficient to replace biopsy. However, it suggests that sonoelastography may be a useful tool to guide biopsies.

V. Conclusion

This study shows a comparison in prostate cancer detection performance between *in vivo* and *ex vivo* sonoelastography. After evaluating 10 patients, sonoelastography showed similar performance for both types of experiments (over 80% accuracy for tumors larger than 4 *mm* in diameter). These results are an improvement over US B-mode but not yet sufficient to replace biopsy. However, these results also imply that sonoelastography has the potential to become an imaging tool to guide biopsy.

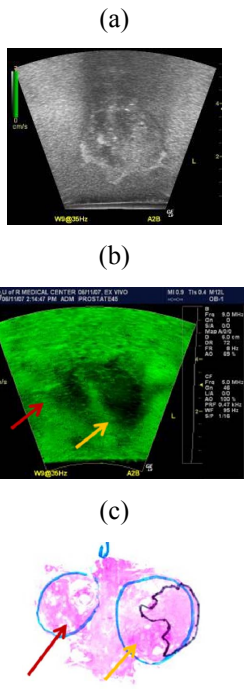

Figure 2. Corresponding (a) B-mode US image, (b) sonoelastographic image, and (c) histological image from an *ex vivo* prostate case. The sonoelastographic image depicts two deficits to the right and to the left of the gland (shown in red and yello arrows). These deficits correspond to BPH nodules and to a cancerous tumor.

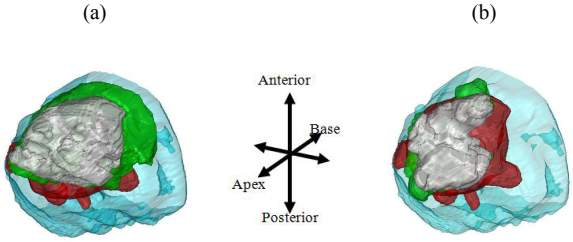

Figure 3. Comparison between sonoelastographic volumes and histology for *ex vivo* (a) and i*n vivo* (b) data. In both cases the deficit found by sonoelastography is shown in green, the tumor outlined in histology is shown in red, and the intersection of sonoelastography and histology is shown in white.

REFERENCES

[1] American Cancer Society - Cancer Facts and Figures 2008, American Cancer Society, 2008.

[2] Instituto Nacional de Enfermedades Neoplásicas - Cuadro estadístico de Neoplasias malignas en hombres 1997-2002, 2002.

[3] A. Reissigl, J. Pointner, H. Strasser, O. Ennemoser, H. Klocker, and G. Bartsch, "Frequency and clinical significance of transition zone cancer in prostate cancer screening," Prostate, vol. 30, pp. 130–135, 1997.

[4] M.C. Benson and C.A. Olsson, "Prostate specific antigen and prostate specific antigen density: Roles in patient evaluation and management," Cancer, vol. 74, pp. 1667-1673, 1994.

[5] W.J. Ellis and M.K. Brawer, "The significance of isoechoic prostatic carcinoma," J. Urol., vol. 152, pp. 2304–2307, 1994.

[6] L.S. Taylor, D.J. Rubens, B.C. Porter, Z. Wu, R.B. Baggs, P.A. di Sant'Agnese, et al., "Prostate cancer: Sonoelastography for in vitro detection", Radiology, vol. 237, pp. 981-985, 2005.

[7] L. Gao, K.J. Parker, R.M. Lerner, and S.F. Levinson, "Imaging of the elastic properties of tissue - A review," Ultrasound Med. Biol., vol. 22, pp. 959-977, 1996.

[8] J. Ophir, S.K. Alam, B. Garra, F. Kallel, E. Konofagou, T. Krouskop, and T. Varghese, "Elastography: Ultrasonic estimation and imaging of the elastic properties of tissues," Proc. Instn. Mech. Engrs., vol. 213, pp. 203-233, 1999.

[9] J. Greenleaf, M. Fatemi, and M. Insana, "Selected methods for imaging elastic properties of biological tissues," Annu. Rev. Biomed. Eng., vol. 5, pp. 57-78, 2003.

[10] A. Lorenz, H. Sommerfeld, M. Garcia-Schurmann, S. Philippou, T. Senge, and H. Ermert, "A new system for the acquisition of ultrasonic multicompression strain images of the human prostate in vivo," IEEE Trans. Ultrason. Ferroelec. Freq. Contr., vol. 46, pp. 1147-1153, 1999.

[11] A. Pesavento, and A. Lorenz, "Real time strain imaging and in vivo applications in prostate cancer," Proc. IEEE Ultrason. Symp., vol. 2, pp. 1647-1652, 2001.

[12] R. Souchon, O. Rouviere, A. Gelet, V. Detti, S. Srinivasan, J. Ophir, and J.Y. Chapelon, "Visualisation of HIFU lesions using elastography of the human prostate in vivo: Preliminary results," Ultrasound Med. Biol., vol. 29, pp. 1007-1015, 2003.

[13] R.M. Lerner, K.J. Parker, J. Holen, R. Gramiak, and R.C. Waag, "Sonoelasticity: Medical elasticity images derived from ultrasound signals in mechanically vibrated targets," Acoust. Imaging, vol. 16, pp. 317-327, 1988.

[14] K.J. Parker, D. Fu, S.M. Gracewski, F. Yeung, and S.F. Levinson, "Vibration sonoelastography and the detectability of lesions", Ultrasound Med. Biol., vol. 24, pp. 1937-1947, 1998.

[15] D.J. Rubens, M.A. Hadley, S.K. Alam, L. Gao, R.D. Mayer, and K.J. Parker, "Sonoelasticity imaging of prostate cancer: in vitro results," Radiology, vol. 195, pp. 379-383, 1995.

[16] L.S. Taylor, B.C. Porter, D.J. Rubens, and K.J. Parker, "Three-dimensional sonoelastography: principles and practices," Phys Med Biol, vol. 45, pp. 1477-1494, 2000.

[17] B. Castaneda, K. Hoyt, M. Zhang, D. Pasternack, L. Baxter, P. Nigwekar, A. di Sant'Agnese, J. Joseph, J. Strang, D.J. Rubens, K.J. Parker, "Prostate cancer detection based on three dimensional sonoelastography," Proceedings of the 2007 IEEE Ultrasonics Symposium, pp. 1353 – 1356.

[18] B. Castaneda, G. Tamez-Pena, M. Zhang, K. Hoyt., K. Bylund, J. Christensen, W. Saad, J. Strang, D.J. Rubens, K.J. Parker, "Measurement of thermally-ablated lesions in sonoelastographic images using level set methods," Proceedings of SPIE, v. 6920, pp. 692018-1 – 692018-8, 2008.

[19] H.M. Ladak, F. Mao, Y. Wang, D.B. Downey, D.A. Steinman, and A. Fenster, "Prostate boundary segmentation from 2D ultrasound images", Med. Phys., vol. 27, pp. 1777-1788, 2000.

[20] B. Castaneda, "Extracting information from sonoelastographic images," Ph.D. Dissertation, University of Rochester, 2009.

[21] M. Zhang, B. Castaneda, Z. Wu, P. Nigwekar, J.V. Joseph, D.J. Rubens, and K.J.Parker, "Congruence of imaging estimators and mechanical measurements of viscoelastic properties of soft tissues," Ultrasound Med Biol., vol. 33, pp. 1617-1631, 2007.

[22] V. Jalkanen, B.M. Andersson, A. Bergh, B. Ljungberg, and O.A. Lindahl, "Resonance sensor measurements of stiffness variations in prostate tissue in vitro - A weighted tissue proportion model," Physiol. Meas., vol. 27, pp. 1373-1386, 2006.

[23] Z. Wu, K. Hoyt, D.J. Rubens, and K.J. Parker, "Sonoelastographic imaging of interference patterns for estimation of shear velocity distribution in biomaterials," J Acoust Soc Am, vol. 120, pp. 535-545, 2006.